Photogenerated-Carrier Collection by Induced Junction and Application to Novel Type of High-Efficiency Si Solar Cell

AUTHOR(S):

FUYUKI, Takashi; MORIUCHI, Sohta; MIYAGAKI, Shinji; MATSUNAMI, Hiroyuki

CITATION:

FUYUKI, Takashi ...[et al]. Photogenerated-Carrier Collection by Induced Junction and Application to Novel Type of High-Efficiency Si Solar Cell. Memoirs of the Faculty of Engineering, Kyoto University 1988, 50(4): 249-261

ISSUE DATE:

1988-11-30

URL:

http://hdl.handle.net/2433/281385

Photogenerated-Carrier Collection by Induced Junction and Application to Novel Type of High-Efficiency Si Solar Cell

by

Takashi FUYUKI, Sohta MORIUCHI, Shinji MIYAGAKI
and Hiroyuki MATSUNAMI

(Received June 30, 1988)

ABSTRCT

A novel type of induced junction (IJ) solar cells to achieve a high efficiency without an n^+ doped layer was proposed. A strong inversion induced by an external bias voltage across an insulating layer yields a very shallow n^+p junction without impurity doping, and heavy doping effects can be taken away. Performances of the IJ cells were discussed in detail, and a conversion efficiency larger than 20% could be expected. A cell-fabrication process was outlined including formation of a charge-collection barrier by ion implantation and deposition of a gate insulator with a high dielectric constant. A very low sheet resistance could be realized at a low bias voltage, and the power of the photogenerated current source increased with bias voltage.

1. INTRODUCTION

Extensive efforts have been carried out theoretically and experimentally to obtain high conversion-efficiency solar cells using Si. Not only the improvement of the short circuit current but also the increase of the open circuit voltage are needed, and the reduction of recombination in the bulk and at the surfaces is essential. Rohatgi [1] developed a simplified analytical model to provide a guideline for maximizing the efficiency including the effects of bandgap narrowing [2], Auger recombination [3], and recombination at the cell surfaces. He showed the possibility of a 20% efficiency using a double-layer AR coating and front- and back-surface passivation with SiO_2. Green et al. inserted a thin SiO_2 layer between an emitter layer and current collection electrodes [4] to decrease the recombination at the metal/Si interface, and characterized the performance of the high-efficiency (up to 22%) cell in detail [5]. A high open circuit voltage up to 681 mV was achieved by reducing the dark saturation current in a newly

Department of Electrical Engineering, Kyoto University.

devised cell whose junction was a set of small point contacts [6]. The conventional high-efficiency cells mentioned above use n^+p junctions to make an internal electric field for charge collection. Hence, heavy doping effects in emitters cause inevitable difficulties, such as a saturation current increase by bandgap narrowing and a lifetime reduction by the Auger recombination.

Recently, silicon inversion layer solar cells have been widely investigated to obtain high conversion efficiencies by low temperature processes without formation of n^+p junctions. High efficiencies up to 17.5 and 13.3% under AM1 illumination have been realized using single- and poly-crystalline silicon wafers, respectively [7, 8]. We have revealed the current transport mechanisms and showed that a strong inversion is needed to decrease the sheet resistance and increase the efficiency [9, 10].

In this study, we propose a novel type of induced junction (IJ) solar cell to achieve a high efficiency without an n^+ doped layer for a charge separation barrier. A strong inversion, induced by an external bias voltage across an insulating layer, yields a very shallow n^+p junction without impurity doping, and the heavy doping effects can be taken away. In contrast to conventional inversion layer solar cells [7] (the inversion layer is formed by fixed charges incorporated in a deposited transparent film), a strong inversion can be obtained, which realizes a very low sheet resistance. First, the basic operation mechanisms are mentioned, followed by a detailed theoretical calculation of the performance of the IJ solar cell. The reduction of the reverse saturation current is shown for the IJ cell in comparison with conventional n^+p junction cells. Optimization of the cell configuration is discussed, and a conversion efficiency larger than 20% can be expected under AM1 (100 mW) illumination. Some experimental results are also described.

2. STRUCTURES AND OPERATION MECHANISMS

The basic structure of the IJ cell is shown in Fig. 1. On the semiconductor surface with current collection electrodes, an insulator of about 100 nm thick is deposited. A transparent conducting film is used as a gate electrode. The current collection electrode is formed with either an n^+p junction or a Schottky barrier with a very thin oxide between the metal and the semiconductor. The inversion layer is induced by applying gate bias voltage V_g, and a very low sheet resistance can be achieved in the strong inversion mode. Using an insulator with a high dielectric constant, a very low sheet resistance less than 1 kΩ/Sq can be obtained by a relatively low applied voltage ($V_g = 3-4$ V). As will be

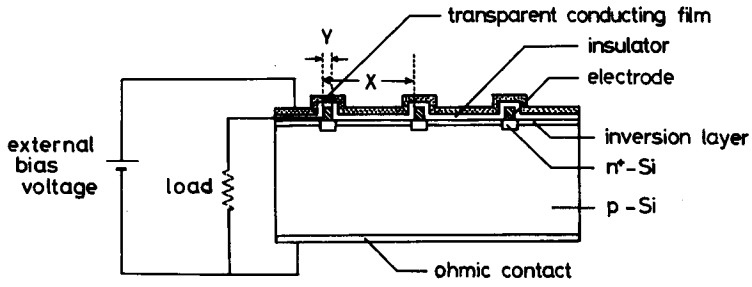

Fig. 1 Cross sectional view of induced junction (IJ) solar cell.

mentioned later, this yields a high conversion efficiency even if the distance X (see Fig. 1) between the grid electrodes is relatively large. In the external bias circuit, the current flow is extremely small, and hence only a small part of a solar cell module can be applied for the voltage source of the bias circuit. The energy loss in the bias circuit can be neglected (lower than 1 % of the total output) if the resistivity of the insulator is larger than 10^{10} Ωcm.

The induced junction solar cell has the following notable features [11]; i.e. 1) A very shallow charge-collection barrier can increase the sensitivity in the short wavelength region, 2) A very low dark saturation current increases the open circuit voltage, 3) Due to a very low sheet resistance, coarse grid electrodes can be used to increase the active area for solar illumination. In the later sub-sections, we will explain these merits in detail.

2. 1 Shallow junction

The "internal" spectral response, (i.e. reflection of light from the surface is assumed to be zero), defined as the number of collected carriers per incident photon at each wavelength was computed using the following well-known equations [12] derived from the continuity equation.

$$\frac{J_p}{qF}=\left[\frac{aL_p}{a^2L_p^2-1}\right]\times\left[\frac{\left(\frac{S_pL_p}{D_p}+aL_p\right)-e^{aw_n}\left(\frac{S_pL_p}{D_p}\cosh\frac{w_n}{L_p}+\sinh\frac{w_n}{L_p}\right)}{\frac{S_pL_p}{D_p}\sinh\frac{w_n}{L_p}+\cosh\frac{w_n}{L_p}}-aL_pe^{-aw_n}\right], \tag{1}$$

$$\frac{J_n}{qF}=\left[\frac{aL_n}{a^2L_n^2-1}\right]\times e^{-a(w_n+w_{dr})}\times\left[aL_n-\frac{\frac{S_nL_n}{D_n}\left(\cosh\frac{W'}{L_n}-e^{-aW'}\right)+\sinh\frac{W'}{L_n}+aL_ne^{-aW'}}{\frac{S_nL_n}{D_n}\sinh\frac{W'}{L_n}+\cosh\frac{W'}{L_n}}\right], \tag{2}$$

$$\frac{J_{dr}}{gF}=e^{-\alpha w_n}[1-e^{-\alpha w_{dr}}]\,, \tag{3}$$

where

α : absorption coefficient
W : total cell thickness
w_n : thickness of n^+ layer and equal to junction depth.
w_{dr}: thickness of depletion region
W': parameter equal to $W-(w_n+w_{dr})$
D_p : diffusion constant of hole
D_n : diffusion constant of electron
L_p : diffusion length of hole
L_n : diffusion length of electron
S_p : surface recombination velocity of hole on top n^+ surface
S_n : surface recombination velocity of electron on rear surface
F : number of incident photons per unit area per unit bandwidth per sec

The responses in typical cases of conventional n^+p and IJ solar cells are shown in Figs. 2 and 3, respectively. The three components J_p, J_{dr}, and J_n collected from the n^+ top layer, the depletion region, and the p-type region are shown by solid, dotted, and dashed lines, respectively. The resistivity of the p type substrate was 0.1 Ωcm, and the diffusion length of the minority carrier (electron) was taken as 125 μm. The thickness of the substrate was 500 μm. The surface recombination velocity varied in the range of 10^3-10^5 cm/sec. For the conventional n^+p cell, the junction depth w_n was chosen as 0.2 μm, and L_p and D_p were assumed to be 0.14 μm and 0.78 $cm^2\ V^{-1}sec^{-1}$. For the IJ cell, w_n, L_p and D_p were taken as 0.01 μm, 2.8 μm, and 2.3 $cm^2V^{-1}sec^{-1}$ under the typical strong inversion condition.

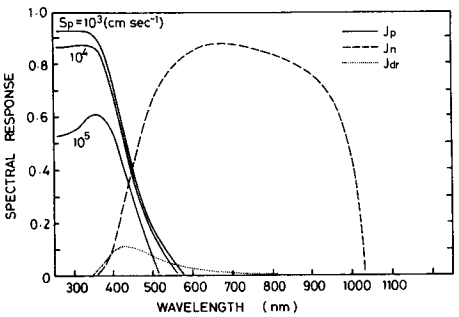

Fig. 2 Internal spectral response of conventional n^+p junction cell.

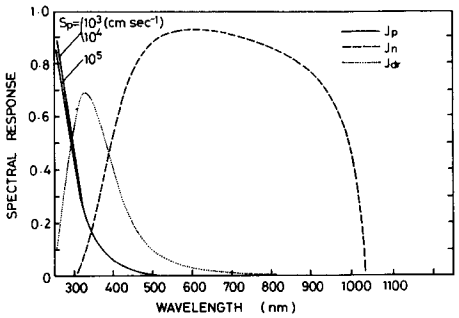

Fig. 3 Internal spectral response of induced junction (IJ) cell.

In the case of the n^+p junction cell, the hole current collected from the surface n^+ layer mainly contributes to the photocurrent in the short wavelength region. Hence, the surface recombination has serious effects on the spectral responses. The response in the range of 250 – 450 nm decreases with increasing S_p as shown in Fig. 2. In the case of the IJ cell, the current collected from the depletion region mainly contributes to the photocurrent, and the surface recombination has no serious influence on the response as shown in Fig. 3. The difference of the surface recombination effects on J_p between the n^+p and IJ cells is caused by the different depths of the charge separation barriers. For the IJ cell, the barrier is made just under the surface, since the thickness of the inversion layer is less than 0.01 μm. On the other hand, the junction depth of the n^+p cell is about 0.1 – 0.2 μm in the practical cell configuration at present.

2. 2 Dark saturation current

Dark saturation currents J_{n0} and J_{p0} due to electrons in the p–Si substrate and holes in the n^+–Si layer were calculated according to the following equations approximately derived by the expression in ref. 13. It was assumed that the thickness of the n^+ layer was very much thinner than the hole diffusion length, and the thickness of the substrate was sufficiently large compared with the electron diffusion length.

$$J_{n0}=qn_{ie}^2\frac{d_n}{L_n N_A(\rho)}, \tag{4}$$

$$J_{p0}=q\frac{n_{ie}^2}{N_D}\left[S_p+\frac{w_n}{\tau_p}\right], \tag{5}$$

where N_A (ρ) and N_D are the acceptor concentration of the substrate (a function of resistivity ρ) and the donor concentration of the n^+ layer. The diffusion length L_n is considered to be a function of ρ, and the values reported in ref. 14 were used in the calculation. The lifetime of minority carriers in the n^+ layer (hole) τ_p was estimated taking the Auger effect into account [15]. The effective intrinsic carrier density n_{ie} was derived by considering the bandgap narrowing effect [16].

The dependence of J_{p0} on the surface recombination velocity S_p is shown in Fig. 4 for various values of N_D (solid lines). The value of w_n is chosen as a typical value of 0.2 μm. Figure 4 also shows J_{n0} for several substrate resistivities (dashed lines). When N_D is comparatively small ($< 10^{18}\,cm^{-3}$), J_{p0} strongly depends on S_p. However, when N_D becomes larger ($> 10^{19} - 10^{20}\,cm^{-3}$), J_{p0} is not influenced by S_p so much, and closes at a certain value ($5 \times 10^{-13}\,Acm^{-2}$) owing to the heavy doping effects. In the case of the IJ cell, the n^+ area is formed only

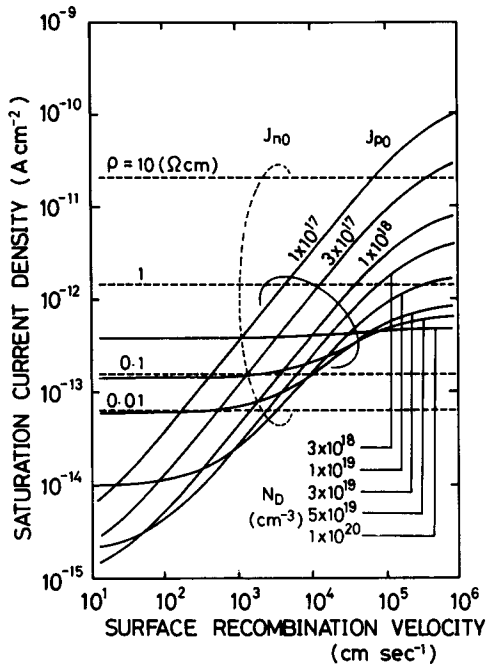

Fig. 4 Reverse saturation current as a function of surface recombination velocity.

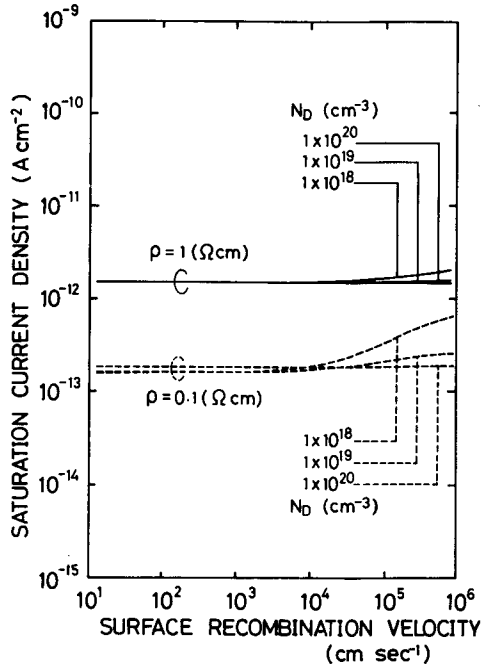

Fig. 5 Total reverse saturation current as a function of surface recombination velocity.

under the current collection electrode, and most of the surface is covered by the induced inversion layer, in which holes don't exist. Therefore, J_{p0} from the inversion layer is considered to be zero, and the component from the n^+ layer under the current collection electrode is taken into account in the estimation of J_{p0}.

The dependence of J_0 on S_p is shown in Fig. 5 for a typical value of $k = 0.06$, where k is the ratio of the electrode area and the total area. Because of the small value of k, J_0 becomes almost equal to J_{n0}. Then, J_0 is constant for various N_D in the range of $S_p < 10^4$ cmsec^{-1}, and is as low as 1.5×10^{-13} Acm^{-2} which is 1/5 of the n^+p junction cell for the same doping levels ($N_D = 10^{20}$ cm^{-3}, $\rho = 0.1$ Ωcm).

2. 3 Sheet resistance

The sheet resistance is expressed as follows:

$$R_{Sq} = [\mu_{eff}(Q_s - Q_A - Q_{ss})]^{-1}, \quad (6)$$

where Q_s is the surface charge density derived from the surface potential Ψ_s (V_g), and Q_A is the acceptor density in the depletion layer. The interface state

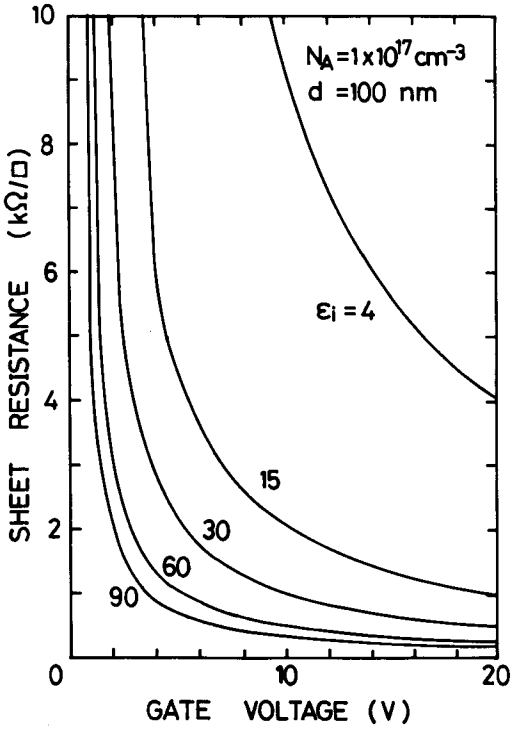

Fig. 6 Dependence of sheet resistance on gate bias voltage.

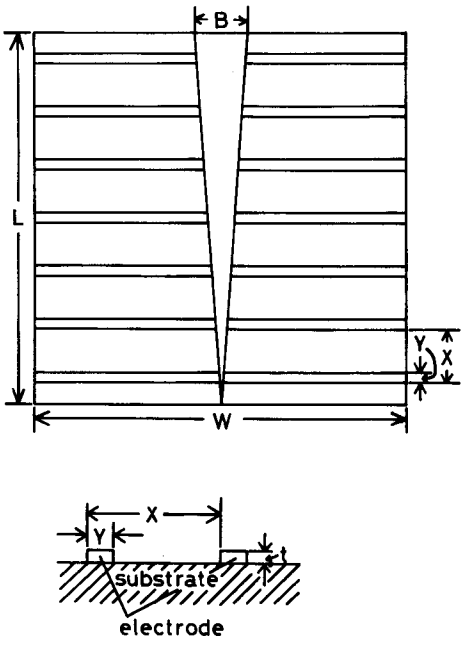

Fig. 7 Grid electrode pattern used in the theoretical calculation.

density Q_{ss} can be neglected since it is less than 1 / 10 of Q_s of the order of 10^{13} cm^{-2}. The expected sheet resistance was calculated as a function of V_g under the following assumptions.

(1) The thickness of the gate insulator is 100 nm and its relative dielectric constant varies from 4 to 90. The use of the large dielectric constant is to obtain strong inversion under low bias voltage.

(2) The effective electron mobility μ_{eff} in the inversion layer is taken as 400 $cm^2V^{-1}sec^{-1}$ which is smaller than that in a bulk. It can clearly be seen in Fig. 6 that a very low sheet resistance smaller than 1 kΩ/Sq can be obtained under relatively low (4 - 8 V) bias voltage if the dielectric constant of the insulator is large (50 - 90).

The conversion efficiency was calculated following the output power equation [17] as a function of the current collection electrode period X (see Fig. 7) with a fixed electrode width Y (see Fig. 7) of 10 μm for various values of J_0.

$$P=|IV|=I\left[\frac{kT}{q}\ln\left(\frac{I+I_L}{I_0}+1\right)+IR_s\right], \tag{7}$$

where I_0 is the total dark saturation current considering the cell configuration. The series resistance R_s was estimated by the simple geometrical calculations using the sheet resistance R_{Sq} of inversion layer and the resistivity of electrode metal. I_L is the power of photo-generated current source, and is nearly equal to a short circuit current in cases of sufficiently small series resistances. The cell size is taken as 1×1 cm^2. In Fig. 8, the solid and dashed lines are the efficiencies for the active and the total areas, respectively, under AM 1 (100 mW) illumination. The short circuit current is assumed to be 37 mAcm^{-2}, which is a typical value under AM 1 (100 mW) illumination. The sheet resistance in the inversion layer is 1 kΩ/Sq. The resistivity (2.74×10^{-6} Ωcm) and the thickness (3 μm) of the electrode metal (Al) are taken into accout in the calculation of the series resistance. Figure 8 clearly shows that the maximum conversion efficiency for the total area is expected as 20 and 18% for $J_0 = 10^{-13}$ and 10^{-12} Acm^{-2}, respectively. If the short circuit current increases 40 mA cm^{-2} by AR coating and surface passivation, a higher efficiency will be obtained.

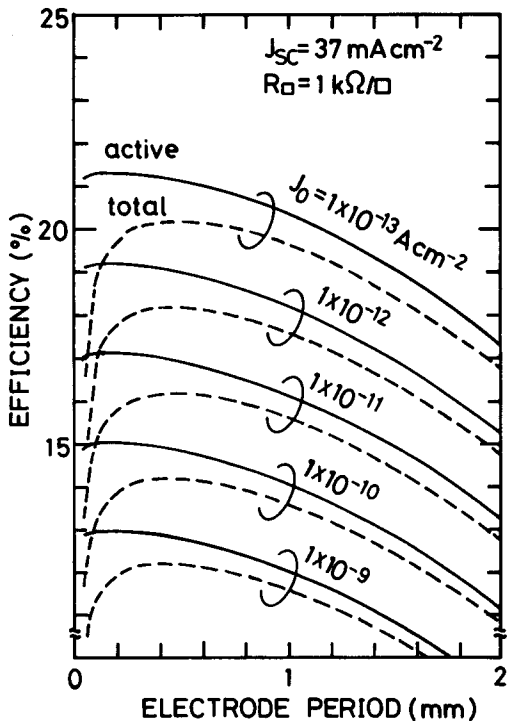

Fig. 8 Dependence of the conversion efficiency of induced junction (IJ) cell on the current collection electrode period.

3. CELL FABRICATION AND ITS PERFORMANCE

Mirror polished (100) surfaces of p-Si (Fz) with the resistivity of 0.1 - 10 Ωcm were used. The outline of a cell fabrication process is shown in Fig. 9. The grids of n^+p charge collection barriers were made by a selective ion implantation technique using a SiO_2 mask. The dosing energy and the level of P^+ ions were 100 keV and $5 \times 10^{14}\,cm^{-2}$, respectively. Almost all impurities were activated after annealing at 800° C for 1 min. After the deposition of a metal electrode (Ti/Ag), a uniform TiO_2 this film was deposited by thermal decomposition of tetra-iso-propyl-titanate (Ti $(OC_3H_7)_4$) at substrate temperatures of 200 - 400° C. A transparent conductive ITO film was deposited by electron beam evaporation

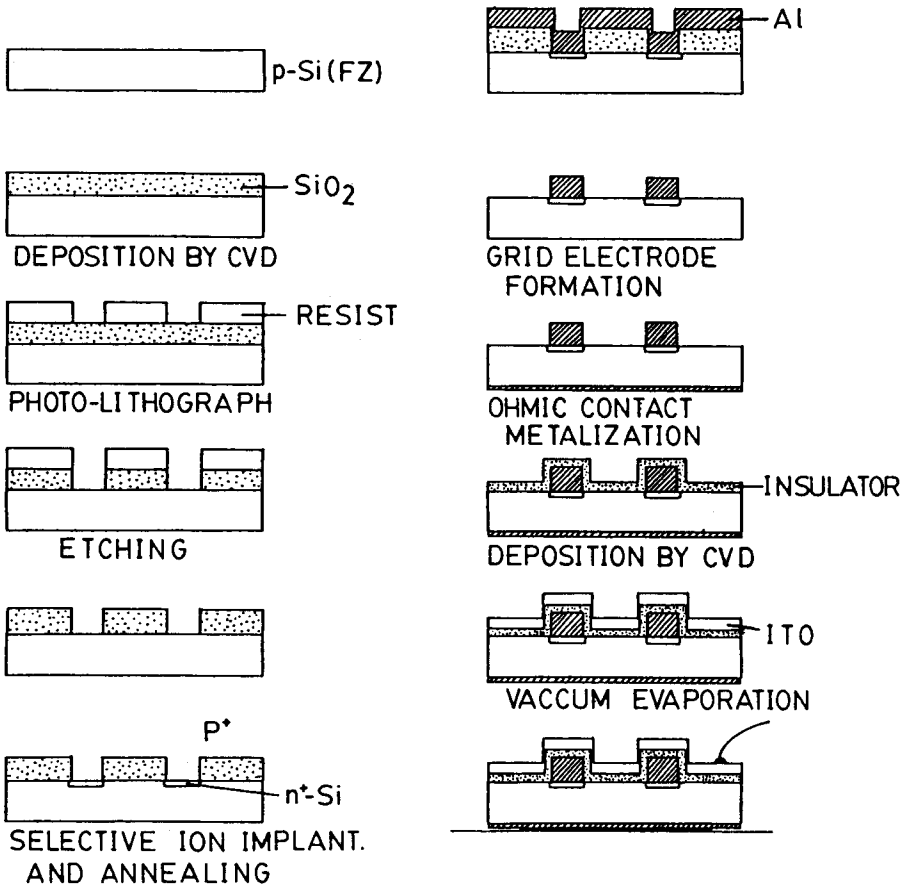

Fig. 9 Outline of cell-fabrication process.

to made an IJ cell.

The gate insulator film needs the following factors: (1) a large dielectric constant to made a strong inversion by low gate bias voltage, (2) a large resistivity to reduce the power loss in the gate circuit, (3) a good transmittance in the visible wavelength region to obtain a high efficiency. The dielectric constant and the resistivity of TiO_2 film made by CVD are 20-86 and 10^9-10^{10} Ωcm [15], and the trasmittance is larger than 85%. Thus, the TiO_2 film is one of promising candidates as the gate insulator of the IJ cell.

The sheet resistance in the inversion layer could be estimated by the dependence of the channel conductance on the channel length in FET (field effect transistor) structures, taking the electrode resistance into account [18]. Figure 10 shows the dependence of the sheet resistance as a function of V_g. The substrate was a p-type wafer with $N_A = 10^{17}\,cm^{-3}$. A thin TiO_2 film whose thickness and relative dielectric constant were 78 nm and 42 was used as a gate insulator. The solid line is the experimental result, and the dashed curve is the theoretical one

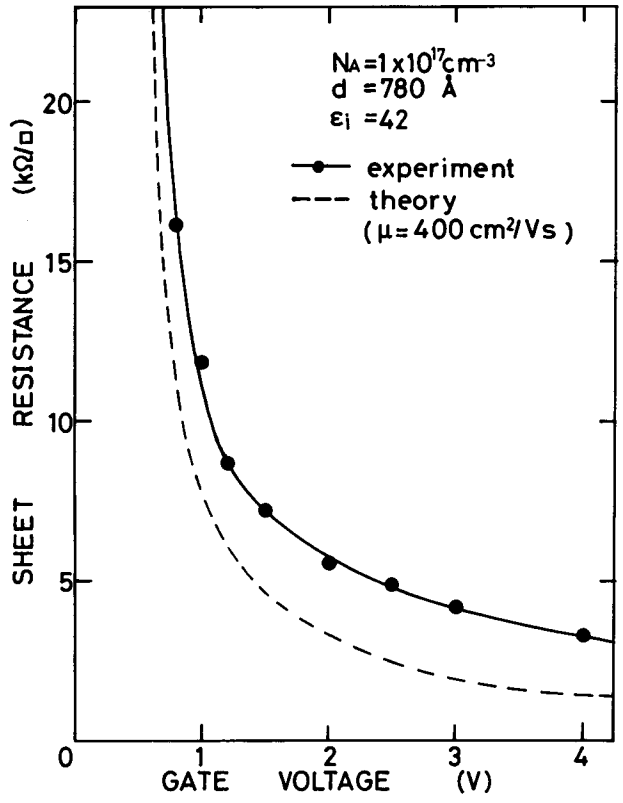

Fig. 10 Dependence of the sheet resistance on gate bias voltage.

using an assumption of $\mu_{eff}= 400\,cm^2V^{-1}sec^{-1}$. The sheet resistance was larger than 10 kΩ/Sq below $V_g= 1$ V, and it decreased rapidly with increasing V_g. The minimum sheet resistance was 3.3 kΩ/Sq at $V_g= 4$ V, which showed that a strong imversion occurred. The experimental values were about twice as large as the theoretical values. This is discussed elsewhere [19].

The photoresponses were measured in the samples with a 1 cm^2 area. A highly resistive SiO_2 of the order of $10^{15\text{-}16}$ Ωcm was used as a gate insulator in order to reduce the power loss in the gate circuit. Fig. 11 shows the dependence

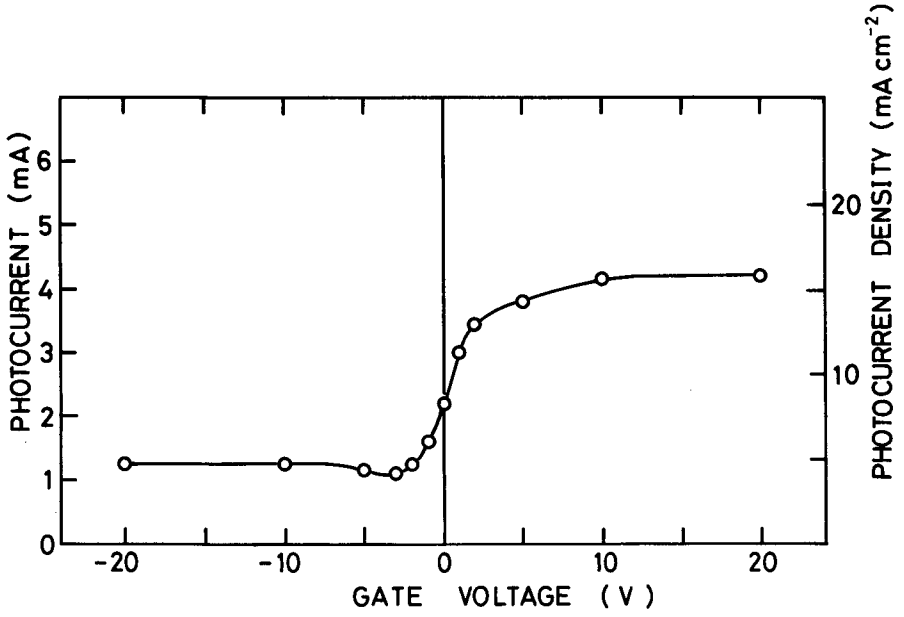

Fig. 11 Saturation photocurrent as a function of gate bias voltage.

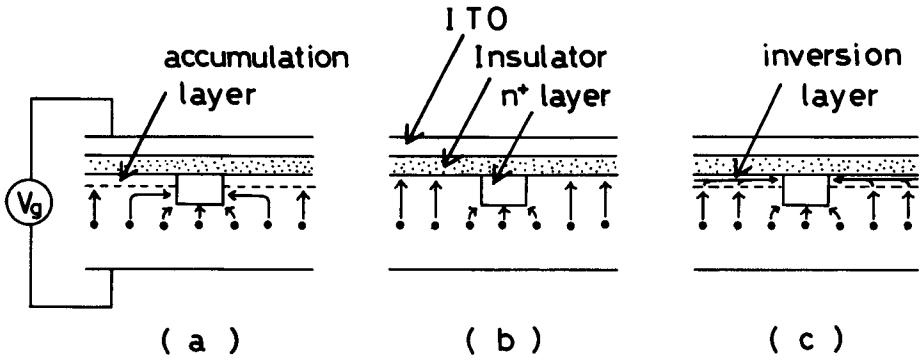

Fig. 12 Collection modes of photogenerated carriers under various bias voltages.

of the power of the photo-generated current source I_L on V_g. I_L was low in the range of $V_g = -1$ V, and it increased rapidly up to 16 $mAcm^{-2}$ with increasing V_g. The surface was in the accumulation or flat band conditions for $V_g = -1$ V. The photogenerated carriers were recombined before they diffused to the charge collection electrodes (Fig. 12 (a) and (b)). For $V_g = 4$ V, a strong inversion occurred, and photogerated carriers could be collected through the inversion layer (Fig. 12 (c)). The operation of the novel type induced-junction cell was confiirmed. A higher photo-generated current will be expected when AR coating and/or back surface field configuration are adopted.

4. CONCLUSION

In this study, we proposed novel type induced junction (IJ) solar cells to achieve a high efficiency without an n^+ doped layer. A strong inversion layer, induced by an external bias voltage across an insulating layer, yields a very shallow n^+p junction without impurity doping, and heavy doping effects can be taken away. Performances of the IJ cells were discussed in detail, and a conversion efficiency larger than 20 % can be expected, owing to a very low dark saturation current compared with that of conventional n^+p junction cells. A cell -fabrication process was outlined, including the formation of a charge-collection barrier by ion implantation, and the deposition of a gate insulator with a high dielectric constant. A very low sheet resistance of about 3 kΩ/Sq could be realized at a low biasd voltage, and the power of the photo-generate current source increased with bias voltage. The IJ cell can be expected ad a promising one of the high-efficiency solar cells.

REFERENCES

1) A. Rohatgi, and P. Rai-Choudhury: IEEE Tran. Electron Devices, **ED-33**, 1 (1986).
2) H. P. D. Lanyon, and R. A. Tuft: IEEE Trans. Electron Devices, **ED-26**, 1014 (1979).
3) J. D. Beck an Conradt: Solid State Communications **13**, 93 (1973).
4) M. A. Green, A. W. Blakers, Shi Jiqun, E. M. Keller, and S. R. Wenham: IEEE Trans. ElctronDevices **ED-31**, 679 (1984).
5) M. A. Green, Z. Jianhua, A. W. Blakers, M. Taouk and S. Narayanan: IEEE Electron Devices **EDL-7**, 583 (1986).
6) R. A. Sinton, Y. Kwark, J. Y. Gan, and R. M. Swanson; IEEE ElectronDevice LeTters **EDL-7**, 567 (1986).
7) R. B. Godfrey, and M. A. Green: Appl. Phys. Lett. **34**, 790 (1979).
8) R. B. Godfrey, and M. A. Green: Jpn. J. Appl. Phys. **19 Suppl. 19-1**, 533 (1980).
9) H. Matsuura, S. Nishino, and H. Matsunami: Jpn. J. Appl. Phys. **20 Suppl. 20-2**, 51 (1981).

10) H. Matsuura, J. Fujii, H. Takai and H. Matsunami: Jpn. J. Appl. Phys. **21 Suppl. 21-2**, 117 (1982).
11) T. Fuyuki, S. Miyagaki and H. Matsunami: Proceedings of the 2nd International photovoltäic Science and Engineering Conference, Beijing, p. 241 (1986).
12) H. J. Hovel; "Solar Cells" (Semiconductors and Semimetals, Vol. 11, Academic Press, New Youk, 1975) pp. 17-20.
13) ibid. P. 51.
14) M. Wolf: Proceeding of the 16th IEEE Photovoltaic Specialists Conference, p. 355 (1982).
15) J. Dzjewior, and W. Schmid: Appl. Phys. Lett., **31**, 346 (1977).
16) J. W. Slotboom, and H. C. De Graaff: Solid State Electronics, **19**, 857 (1976).
17) S. M. Sze; "Physics of Semiconductor Devices, 2nd edit." (John Wiley, and Sons, New York, 1981) pp. 806-807.
18) T. Fuyuki and H. Matsunami: Jpn. J. Appl. Phys. **25**, 1288 (1986).
19) T. Fuyuki, S. Moriuchi, and H. Matsunami: Technical Digest of the International PVSEC-1, Kobe, P. 763 (1984).